Journal of Membrane Science and Research 7 (2021) 173-184

Journal of Membrane Science & Research

journal homepage: www.msrjournal.com

Research Paper

Fresh and Uncalcined Solution Blow Spinning - Spun PAN and PVDF Nanofiber Membranes for Methylene Blue Dye Removal in Water

Shierlyn S. Paclijan [1], Shenn Mae B. Franco [1], Rodrigo B. Abella [1], Jona Crishelle H. Lague [1], Noel Peter B. Tan [2,*]

[1] *Chemical Engineering Department, Xavier University – Ateneo de Cagayan, Corrales Avenue, Cagayan de Oro City, 9000 Philippines*
[2] *Department of Chemical Engineering, University of San Carlos, Nasipit, Talamban, Cebu City, 6000 Philippines*

Article info

Received 2020-03-10
Revised 2020-08-18
Accepted 2020-08-18
Available online 2020-08-18

Keywords

Solution blow spinning
Nanofiber membrane
PAN
PVDF
Methylene blue removal
Adsorption capacity

Highlights

- Cheap, easy to fabricate and direct use of SBS-spun nanofibers for wastewater MB dye absorption.
- "No pre-treatment" use of PAN and PVDF nanofibers as comparatively effective for MB dye removal.
- Investigation of MB initial concentration and adsorption contact time of SBS-spun PAN and PVDF membranes for MB dye removal.
- Investigation of different adsorption isotherms (i.e., Langmuir, Freundlich, and Dubinin-Radushkevich) in predicting the maximum adsorption capacities of SBS-spun PAN and PVDF membranes for MB dye removal.

Graphical abstract

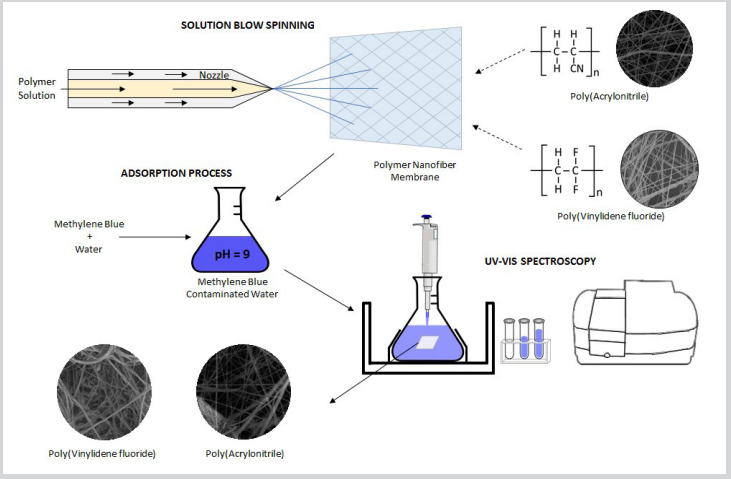

Abstract

Freshly produced and uncalcined solution blow spun-poly (acrylonitrile) (PAN) and poly (vinylidene fluoride) (PVDF) nanofiber (NF) membranes were utilized as adsorptive membranes for methylene blue (MB) dye in water under batch adsorption. The effects of various initial dye solution concentrations (3-15 mg/L) and contact time (1-10 minutes) versus its adsorption capabilities of the nanofiber membranes were studied. Furthermore, adsorption isotherm that best fit the experimental data was determined. The equilibrium adsorption capacity, q_e, for both nanofiber membranes increased with MB concentration of 3 - 7 mg/L but q_e considerably decreased when such MB amounts increased to 15 mg/L. The highest q_e obtained was 50.78 and 34.97 mg/g for PAN NF and PVDF NF membranes, respectively. Both NF membranes also showed high MB adsorption with increased contact time until equilibrium was reached. PAN demonstrated better adsorption capacity compared to PVDF at all levels of initial dye concentrations studied. Both nanofiber membranes are proposed to conform to the Dubinin-Radushkevich adsorption isotherm model. Using this model, the predicted values for the highest adsorption capacity, q_{max}, of PAN and PVDF NF membranes are 55.91 mg/g and 44.06 mg/g, respectively.

1. Introduction

Dyes are organic compounds used by many industries that require coloring in their products such as in fabrics, food and beverages, and papers. With the increasing rate of industrialization, the usage of these dyes sequentially increases the release of dye waste in land and bodies of water [1]. Among these organic dyes produced, methylene blue (MB) is utilized in many products such as silk, cosmetics, and both in chemical and biological laboratory procedures. Even though it is not actively hazardous, harmful effects to humans are inevitable. These effects include vomiting, increased heart rate, Heinz body formation, cyanosis, quadriplegia, jaundice, and tissue necrosis [2].

Various way to remove dyes in solutions, are categorized into three parts, namely biological, chemical, and physical means. Biological methods such as aerobic processes, anaerobic processes, or a combination of both are commonly used techniques in the removal of dye from bodies of water. However, these processes require strict operating conditions and are less efficient in dye removal [3]. Chemical methods, on the other hand, are based on electrochemical oxidation, advanced oxidation, and photocatalysis of dyes. Significant drawbacks of these processes include the requirement of highly efficient oxidative catalysts and the need for an additional oxidative agent [4]. Physical methods involve membrane separation technologies and adsorption methods. Among the physical techniques, adsorption has remained to be the widely used techniques toxic trace metals and persistent organic micro-

* Corresponding author:E-mail address: noelpetert@gmail.com; npbtan@usc.edu.ph (N.P.B. Tan)

DOI: 10.22079/JMSR.2020.122267.1356

pollutants removal from water. It is a superior technique considering its cost, design, and operation [5].

The use of nanofiber membranes is widely popular nowadays due to its chemical nature, surface polarity, surface area, and structure. These unique characteristics influence the attractive force between the adsorbate and adsorbent [6]. Numerous ways are developed to fabricate nanofiber membranes. These methods include solution intercalation [7], centrifugal spinning [8], melt blowing [9], and electrospinning [10]. However, these methods have their drawbacks, such as usage of large amounts of organic solvents and limited for specific polymer/solvent pairs [7] for solution intercalation which is environmentally unfriendly, low fiber efficiency for electrospinning [10], and strict thermoplastic polymers precursor for the case of melt blowing. [9] Therefore, there is a need for a more straightforward and economical, yet effective, method in producing nanofiber membranes as adsorbents for industrial wastes. The main advantage of solution blow spinning over the electrospinning method is the high production rate. Such a rate goes over thirty times greater than the conventional electrospinning. Solution blow spinning also does not need electricity to produce nanofibers from the polymer precursor. Compared to electrospinning, it needs high voltage (i.e., 10 – 2- kV), which implies some safety issues. On the other hand, the main disadvantage of this technology is its selectivity of application and the quality of the nanofibers can be different from electrospinning. Solution blow spinning nanofibers may produce bundled nanofibers.

An excellent method of producing the nanofiber membrane has emerged in the past two decades. This process is called Solution Blow Spinning. Such process is a hybrid of both melt-blowing and electrospinning. Solution blow spinning is a relatively new method to sythesize nano to microfibers using polymer solutions without voltage requirements [11]. Such a method deposits more polymers at a rapid rate. It also provides micro to nanosize fibers whose quality is the same as that of electrospinning [12]. Such technology depends on the gas velocity, usually air as a fiber-forming mechanism by blowing substrate solutions into a concentric nozzle to produce nanofibers [13]. Different types of polymer precursors have been used in Solution blow spinning for nanofiber synthesis. Precursors range from synthetic [14] to bio-based and biocompatible sources [15]. Solution blow spinning method has received attention because of its smooth operation with a high production rate [16]. Solution blow spun nanofiber membranes manifest properties such as high surface area-to-volume ration and porosity, capable for different solutions to air [17] and water pollution remediation [12, 18]. Another feature of this technology is that it is able to produce nanofibers with cellulose precursor and ceramic additives. Such ability was demonstrated in the work of Dadol et al. [19] for cellulose with PAN and Tan et al. [20] for TiO_2 and PVP.

In this study, solution blow spinning was used for producing different nanofibers, namely poly (acrylonitrile) and poly (vinylidene fluoride). They are investigated for their potential as adsorbents for MB dye in solutions. PAN and PVDF nanofiber membranes were chosen in this study since these two polymers are commonly used in the production of many commercial membranes. They are also easily fabricated through solution blow spinning technique. These nanofiber materials are similar to those investigated for the efficient capture of PM2.5 when embedded on commercial surgical masks [21]. However, the uncalcined and freshly produced nanofiber membranes were directly used as adsorbents for MB dye. These membranes are unique from other existing adsorption studies since no pretreatments of the membrane were carried out. Therefore this type of membrane production addresses the need for a simple, rapid, and industrially scalable process. There are two significant values in this work. 1) This is the first time that a solution blow spun PAN and PVDF nanofiber membranes were utilized directly for adsorbing MB from simulated water. 2) Results showed that the performance of both fresh and uncalcined PAN and PVDF nanofiber membranes are competitive enough compared to some published performance of different materials for MB adsorption. If published, this research work will be a benchmark for future cost-effective method of nanofiber membrane fabrication for industrial wastewater. Furthermore, this study opens up more opportunities for the development of *in-situ* use of cost effective nanofiber membranes.

2. Experimental

2.1. Materials

Poly (acrylonitrile) (PAN, Mw =150 kDa), Poly (vinylidene fluoride) (PVDF, Mw = 180 kDa), Dimethyl formamide (DMF) and acetone were all purchased from Sigma-Aldrich. Methylene blue (MB), a cationic dye with CI Classification Number of 52015 was obtained from Merteflor Enterprises with brand HiMedia. Sodium Hydroxide (NaOH), CAS-No. 1310-73-2, an alkali metal hydroxide commonly known as caustic soda, was purchased from Merteflor Enterprises branded EMSURE®. The distilled water used branded as Absolute was purchased from local stores.

2.2. Solution blow spinning of PAN and PVDF

Precursor solutions were prepared by mixing 9% (w/v) PAN/DMF and 15% (w/v) PVDF/DMF with acetone by thoroughly mixing and heating above room temperature until a homogenous mixture was reached. Homogeneous precursors were directly fed into the solution blow spinner's inner concentric nozzle with a feed rate of 10 mL/hr. Air at three bars was fed to the inner nozzle of the spray system. The needle used in this set-up was 21G (1.5" and inner diameter of 0.514 mm). A vacuumized rotating drum (i.e., 38 cm. working distance) was used to collect the nanofiber mats produced on a PET as substrate. A similar laboratory set-up was utilized by Salva et al. in spinning cellulose-based (i.e., Carboxymethyl cellulose) polymer forming into unique nanowhiskers [22].

2.3. Preparation of nanofiber adsorbent samples and MB dye solutions

The NF membrane samples were directly cut from the original nanofiber mats. An estimated sample size of 5 cm by 5 cm was used for both NF membranes in the batch adsorption. The PAN and PVDF membrane samples have a mass of 0.00703 g and 0.0082 g respectively. The samples obtained were clean and free from any factors, which would give any unforeseen effect on the withdrawn aliquot concentrations from the MB solution.

Aqueous solution of MB dye was created by mixing 20 mg of methylene blue in 1000 mL of distilled water. Serial dilutions were carried out for the calibration of the UV-Vis Spectrophotometer. Such instrument was used in the determination of the exact MB concentration in every aliquot samples. The initial MB dye concentrations of 3, 5, 7, 10, and 15 (i.e., in mg/L) were investigated under batch adsorption experiments. The methylene blue solution was adjusted to pH 9 prior to this set-up using a 0.1M sodium hydroxide for a more effective adsorption performance of MB [23].

2.4. Batch adsorption set-up

Figure 1 shows the experimental batch adsorption carried out in this study. First, a 150 mL of MB solution with a fixed concentration was mixed into a 250-mL flask and placed in a Model G76 New Brunswick Scientific Gyrotory Water Bath Shaker. The freshly prepared NF membrane was subsequently immersed inside the flask and the shaker rotated from 20 to 400 revolutions per minute (rpm). Aliquots were obtained after 1, 2, 4, 6, 8, and 10 minutes adsorption using a pipette for analysis. Samples obtained at different contact times were analyzed using UV-vis – Merck SpectroQuant® Pharo 300 which quantitatively determines the absorbance of the analyte, which is directly related to its concentration. The same procedure was applied for both types of NF membranes.

2.5. Characterizations

Scanning electron microscopy (SEM) using SEM Hitachi TM3030 Plus at an accelerating voltage of 15kV was used in the examination of the nanofiber morphologies. Nanofiber average diameter and its pore size distribution were carried out using Image J software. Chemical analysis of the PAN and PVDF nanofiber membranes was determined using Fourier transform infrared spectroscopy (FTIR). Thermal analyses such as Thermogravimetric Analysis (TGA) and Differential scanning calorimetry (DSC) of nanofiber membrane was carried out in a Perkin Elmer STA 6000 and Perkin Elmer DSC 4000, respectively. Approximately 10 mg of sample for TGA was heated from 30 to 350°C under N_2 of a flow rate of 20 mL/min. DSC analysis used approximately 6 mg sample on a standard Al pan, heated to 30°C for 5 minutes and subsequently heated to 445°C (i.e.,10°C/minute heating rate) under N_2 atmosphere of 20 mL/min flow rate.

2.6. Adsorption Studies

The amount of adsorption on the membrane at a certain time is defined as the adsorption capacity, and it is numerically expressed as follows [24],

$$q_t = \frac{(C_o - C_t)V}{W} \quad (1)$$

where C_o = initial concentration of MB (mg/L), C_t = concentration of the solution at any time t, W = mass of nanofiber adsorbent (g), and V = volume of sample solution (L).

2.7. Adsorption Equilibrium Isotherm

Adsorption mechanisms are mainly determined by well-established isotherms [25]. Langmuir isotherm and Freundlich isotherms are two of the mostly utilized equations [24,26]. In Langmuir isotherm, chemisorption is the mian mechanism. Such isotherm assumes actives sites on the surface are fixed wherein a monolayer is formed. These actives sites are the ones attracted to the adsorbates, which is a reversible reaction and that reaches equilibrium state [25,27]. Freundlich isotherm, on the other hand, is most useful for physical adsorption particularly for liquids and assumes surface heterogeneity which means that adsorbate forms multilayer on the surface of the adsorbent [25, 26, 28]. The linearized form of the two adsorption isotherms are;

$$\frac{1}{q_e} = \frac{1}{qm} + \frac{1}{bq_m C_e} \tag{2}$$

$$lnq_e = lnK_F + \frac{1}{n_F} lnC_e \tag{3}$$

where *Ce* = the equilibrium concentration of MB (mg/L) at equilibrium, q_e = equilibrium adsorption capacity of NF membrane adsorbents (mg/g), and q_m is the maximum adsorption capacity of the NF membranes. K_F and n_F are the isotherm constant and the intensity of the adsorption respectively [26,29].

Another adsorption isotherm is the Dubinin-Radushkevich model. This model uses a heterogeneous surface of the adsorbent (i.e., NF membrane) for adsorption reaction. Such model further uses a Gaussian energy distribution [30]. The isotherm is expressed in terms of its non-linear form.

$$q_e = q_m e^{-\beta\epsilon^2} \tag{4}$$

where q_e = equilibrium adsorption capacity (mg/g), q_m= adsorption capacity at maximum (mg/g), β = Dubinin-Radushkevich constant, and ∈ = Polanyi potential. A linear form of the equation (eq'n 5) is used in obtaining the maximum adsorption capacity wherein ln q_e vs ϵ^2 is plotted.

$$lnq_e = \ln(q_m) - \beta\epsilon^2 \tag{5}$$

The Polanyi potential is expressed as:

$$\epsilon = RTln\left(1 + \frac{1}{C_e}\right) \tag{6}$$

where *R* = gas constant 8.314 (J* mol-1 *K-1), and T = absolute temperature (K). The mean free energy of adsorption, *E* (kJ/mol), used in identifying the type of adsorption involved is expressed as:

$$E = \frac{1}{(2B)^{\frac{1}{2}}} \tag{7}$$

If the mean free path value is between 8 -16 kJ/mol, chemisorption and ion-exchange are assumed to have happened during adsoprtion. While Physisorption, on the other hand, is assumed if the mean free path value is less than 8 kJ/mol [31].

Plotting $1/q_e$ vs $1/C_e$, ln q_e vs ln C_e, and ln qe vs ϵ^2 for Langmuir, Freudlich and Dubinin-Radushkevich isotherms respectively, allows getting the best fit model for the experimental adsorption data.

3. Results and discussion

3.1. Morphologies of nanofibers and adsorption binding mechanism

The solution blow spinning process produced PAN NF membranes with larger diameters and pore sizes than the PVDF NF membranes as shown in Table 1. This difference in fiber diameter and pore sizes may be attributed to parameters such as polymer content, solution concentration, feeding rate of the prepared polymeric solution, and gas pressure [32].

Table 1
PAN and PVDF nanofiber diameters, pore sizes and porosity.

Nanofiber	Average Diameter (nm)	Average Pore Size (μm)	Porosity (%)
PAN	666.31± 252.8	19	46
PVDF	94.1±4.6	2	34

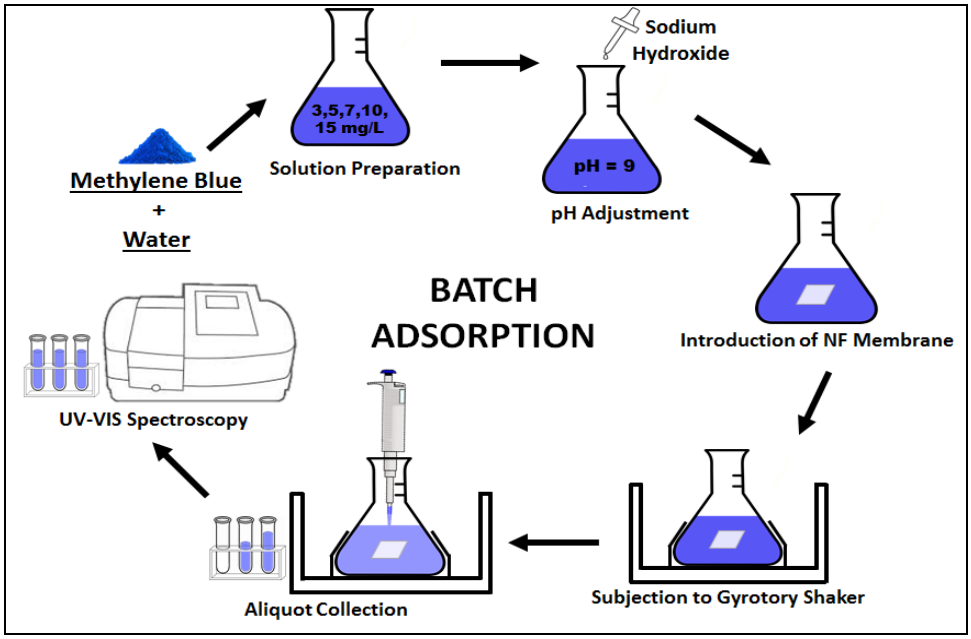

Fig. 1. Batch adsorption set-up.

SEM images of the fresh and uncalcined nanofiber membranes are shown in Figure 2 (i.e., PAN and PVDF nanofibers) for both the before and after adsorption studies. Both PAN and PVDF nanofibers shown in Figures 2a and 2c were used with no prior treatment and showed smooth and uniform fiber diameters. The nanofiber membranes after adsorption (see Figure 2b and d) showed rough fiber surfaces with significant clumping of PVDF nanofibers (Figure 2d). The rough texture is attributed to the MB molecules adsorbed on the nanofiber surface. As observed, nanofiber clumping of nanofibers happen. This is primarily due to the high aspect ratio of the nanofibers coupled with the strong surface adhesion forces [33]. PVDF nanofibers have smaller fiber diameters than the PAN nanofibers (see Table 1), which explains why more clumping can be observed on the former. This clumping reduces the available surface area for MB adsorption resulting in a lower adsorption capacity for PVDF compared to PAN as observed in the succeeding adsorption experiments.

The FTIR analysis of PAN NF membrane (see Figure 3 before) reflects the functional groups of C=C at1629 cm^{-1}, C-H at 1454 cm^{-1}, and 1227 cm^{-1}. The nitrile peak C≡N (2243 cm^{-1}), which should have been a moderately active peak, could not be very well observed in this spectrum [34]. After adsorption however (see Figure 3 after), small nitrile peak is seen on the FTIR analysis of PAN NF membrane, together with the peaks that can be attributed mostly to methylene blue. These peaks include C-S-C at 1095 cm^{-1} and $C=S^{+}$ at 1469 cm^{-1}. PAN nanofibers' nitrile group present is an electron-rich property, which acts as hydrogen bond acceptor [35] while MB has an electron-deficient functionality on its structure at a protonated nitrogen state. The attachment of MB onto the PAN nanofiber membrane then is most likely to occur during the adsorption process through an interaction with the electron-rich PAN and electron-deficient MB. MB molecule absorption on both FTIR Figures 3 and 4 were similar to the study of Pant et al. [36].

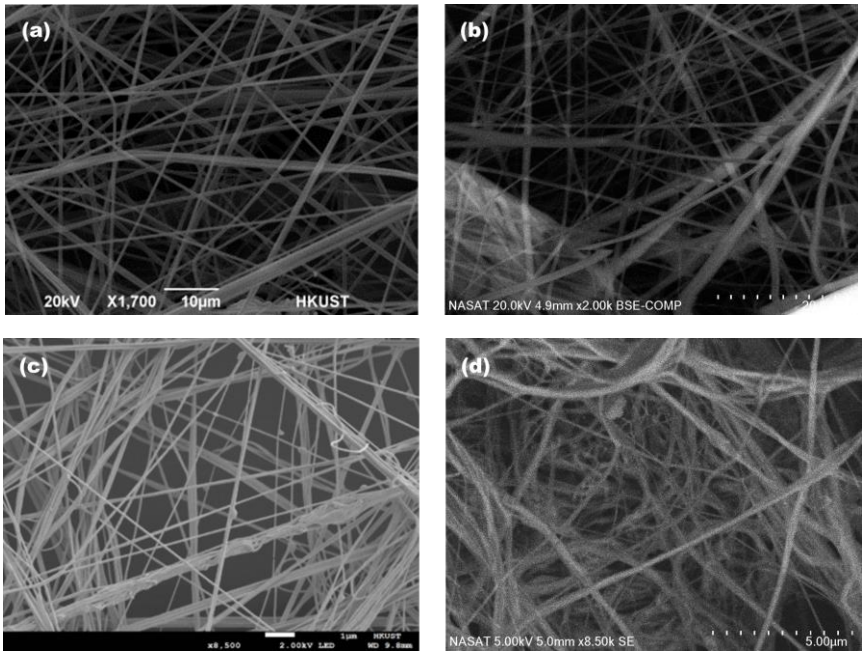

Fig. 2. SEM images of (a) PAN before adsorption, and (b) PAN after adsorption, (c) PVDF before adsorption, and (d) PVDF after adsorption.

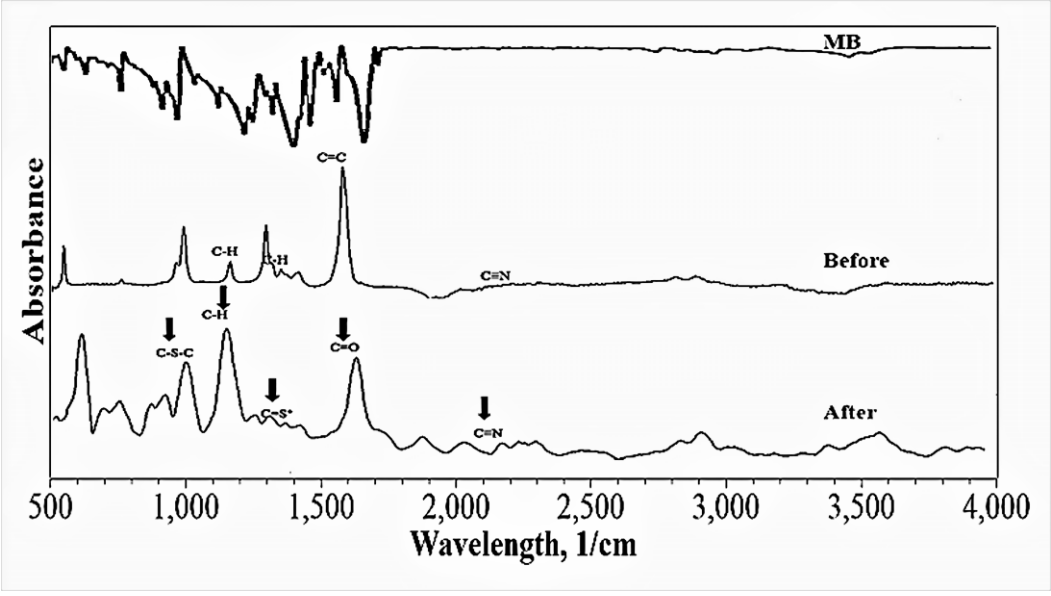

Fig. 3. FTIR Spectrum of PAN nanofiber membrane. Topmost is the MB molecule spectra, middle part is the "before" adsorption studies, and the lowermost part represents "after" adsorption studies on methylene blue

The FTIR analysis in PVDF nanofiber before adsorption (see Figure 4 before) shows the presence of the different molecular functionalities based on their absorption peaks. These absorption peaks include C-H_2 at 3022 cm^{-1}, 2980 cm^{-1}, 1403 cm^{-1}, C-C at 1185 cm^{-1}, C-C-C at 878 cm^{-1}, and C-F at 840 cm^{-1} [37]. After adsorption (Figure 4 after) as in the case of PAN, the peaks attributed to the MB dye such as C-S-C (1076 cm^{-1}) and C-H3 (2919 cm^{-1}, 2850 cm^{-1}) are also detected. Comparing the peaks attributed to C-F (840 cm^{-1}) before and after the adsorption showed a decrease in its intensity, which implies the binding of MB through the fluoride atoms of PVDF nanofiber membrane. The PVDF nanofiber membrane has two fluorine atoms that are arranged symmetrically with a central carbon. The highly electronegative nature of the fluorine atom results in the high-energy bond with the low electronegative functional group (i.e., in the form of nitrogen) present in the methylene blue [38]. The attachment of MB to the surface of the PVDF NF membrane is responsible to this bonding during adsorption.

3.2. Contact time effect

MB adsorption behaviors on both PAN (see Figure 5) and PVDF (see Figure 6) NF membranes showed an initial high rate of adsorption, followed by a slower adsorption rate as contact time is increased. In both PVDF and PAN nanofiber membranes, adsorption is fastest during the first sixty seconds and proceeds more slowly in the next 10 minutes. The fastest adsorption occurred during the first minute because most of the binding sites on the nanofiber surface are still available for adsorption. As contact time is increased, further adsorption is slowed down because of the partial saturation of the active sites on both nanofiber adsorbents. Adsorption rate is expected to further decrease until equilibrium is achieved, that is when the nanofiber active sites are no longer available for binding.

Logarithmic regression is then employed to extrapolate and determine the contact time when the equilibrium is achieved. Results show that the PAN NF membranes is expected to achieve equilibrium after 325.77 minutes, resulting in a q_m of 50.78 mg/g (See *Supporting Information S1*), while PVDF is expected to reach the equilibrium adsorption state after 226.73 minutes with the highest adsorption capacity 34.97 mg/g (See *Supporting Information S2*). The relationship of higher adsorption capacities being made at longer equilibrium contact times is the same for both nanofiber membranes.

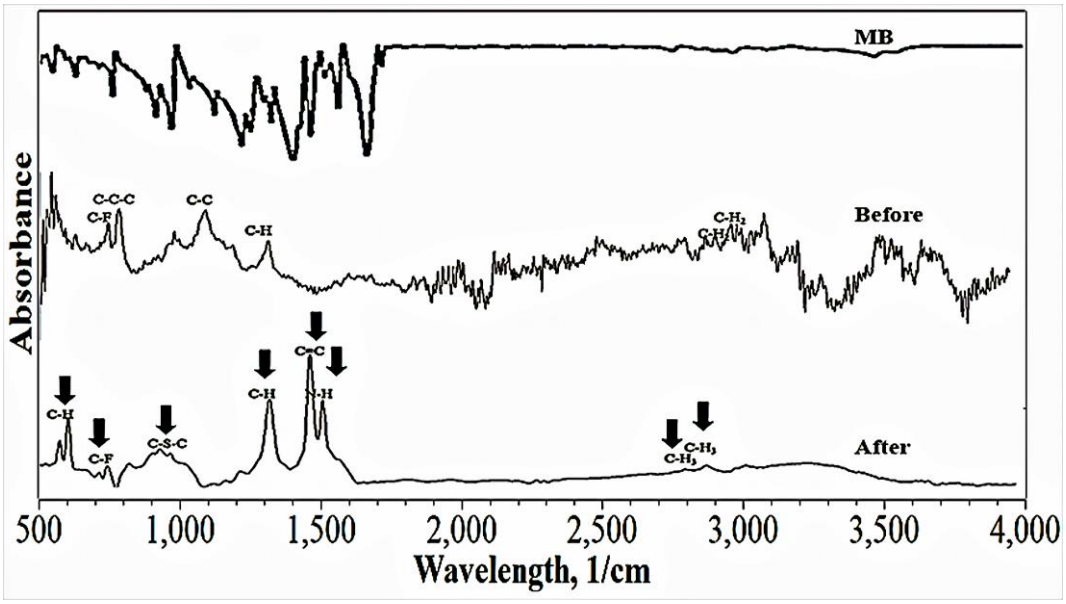

Fig. 4. FTIR Spectrum of PVDF Nanofiber. Topmost is the MB molecule spectra, middle part is the "before" adsorption studies, and the lowermost part represents "after" adsorption studies on methylene blue.

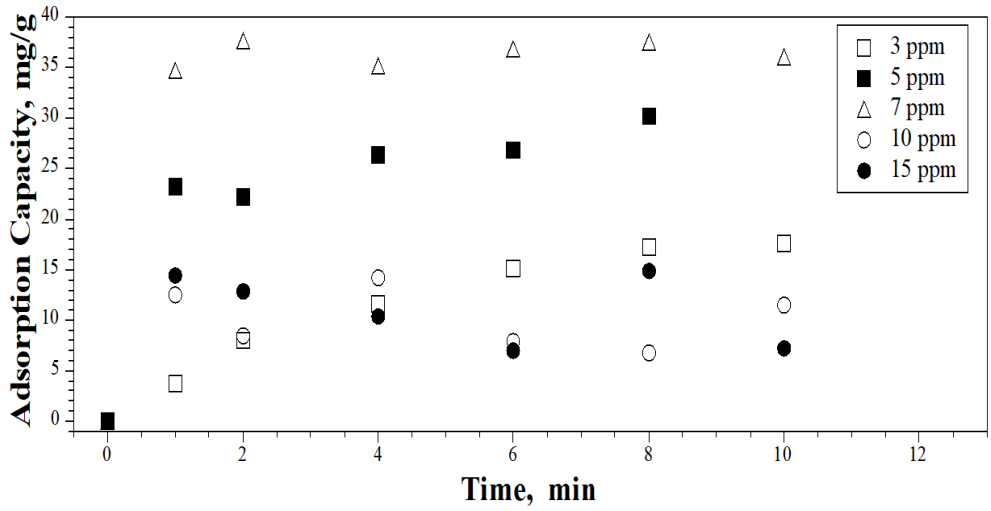

Fig. 5. Adsorption capacities of PAN using different contact time (minutes).

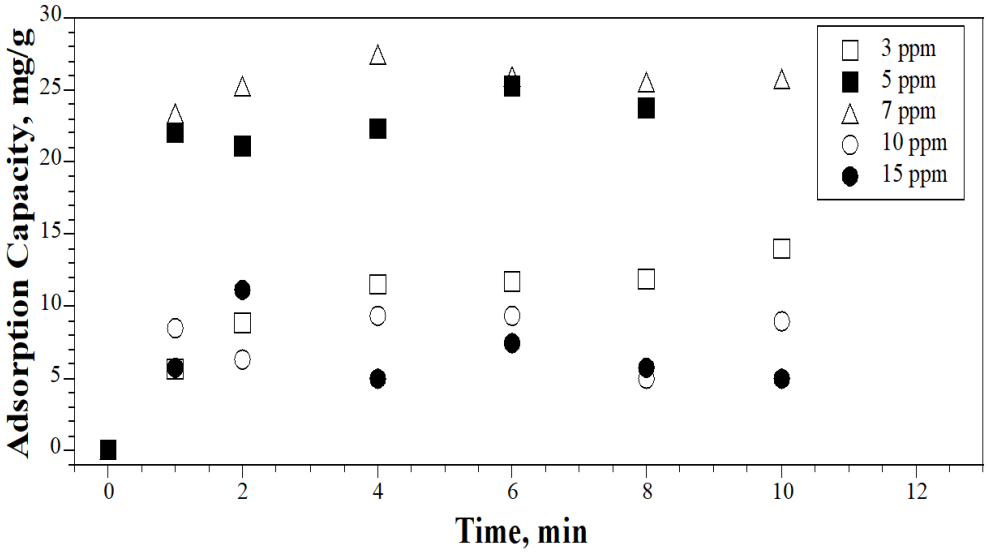

Fig. 6. Adsorption capacities of PVDF using different contact time (minutes).

3.3. Thermal Analyses of PAN membrane

Thermal stability and properties of PAN nanofiber membrane are explored in this study by using Thermal gravimetric analysis (TGA) and differential scanning calorimetry (DSC). The TG-DTG curve in Figure 7a is shown by plotting the percent (%) weight loss versus its corresponding temperature. PAN membrane had a negligible weight loss up to 277 ºC. As the temperature was increased to 950 ºC, the weight loss of the PAN has reached to around 86% leaving a residue of 14%. The peak of mass loss was also observed at 386 ºC. A slight weight loss occurred up to 277 ºC, which signaled that only cyclization was occurring, that should have no weight losses theoretically [39]. Beyond 277 ºC, PAN starts to degrade releasing volatile products such as cyanogen, hydrogen cyanide, acrylonitrile, acetonitrile, and vinylacetonitrile [40]. Aside from the degradation of the PAN nanofiber membrane, an overlap also occurred for the degradation of the PET substrate from 401ºC to 494 ºC [41]. The peak derivative weight loss at 386 ºC was attributed by the overlapping degradation of PAN nanofiber and PET substrate [19].

Figure 7b, on the other hand shows the DSC curve by plotting the heat flow with respect to temperature. In this curve, glass transition temperature and the melting peak (i.e., T_g, and T_m, respectively) are revealed. The melting peak temperature, T_m, is shown in Figure 7b at 257 ºC. The magnified DSC curve in Figure 7c reveals the glass transition temperature, at 83 ºC. Such endothermic observation at a peak of 257 ºC reveals an absorbed heat value of 40 J/g caused by the degradation of the volatile products [40].

3.4. Initial concentration effect

The original MB concentration of the solution significantly affects its adsorption performance for both PAN and PVDF nanofiber membranes (see Figure 8). Increasing the levels of MB from 3-7 mg/L shows that the adsorption capacity of the PVDF NF membrane (i.e., at equilibrium), qe, increases from 14.41 to 34.97 mg/g. The equilibrium adsorption capacity PAN NF membrane also increased from 17.34 to 50.78 mg/g for the same original concentration. Such phenomenon happens because at lower concentrations of MB, fewer MB molecules are available for binding with the large adsorbents' active sites resulting in low equilibrium adsorption. In contrast, at higher MB levels, active sites attract more MB molecules; hence high adsorption capacity is achieved [42]. However, when the original MB level is further increased to 10 mg/L and 15 mg/L, the adsorption capacity decreases to 9.98 mg/g and 11 mg/g for PAN and 12.81 mg/g and 13.88 mg/g, respectively. This sudden decrease is due to the agglomeration of MB molecules in the solution as the concentration is increased. Agglomeration of MB results in a substantial layer of MB-saturated surface of the nanofiber. Such event hinders further adsorption of the MB molecules on the NF membrane and therefore limits its adsorption capacity. Therefore, excess MB molecules remain in the bulk solution and are not further adsorbed on the nanofiber membranes.

A comparison of the adsorption performance of both types of nanofiber showed that PAN NF membrane has higher adsorption capacities at all levels of initial concentration when compared to PVDF NF membranes (see Table 2). Such a phenomenon is caused by the difference in the pore size and porosity of both NF membranes. PAN NF membrane has a larger mean pore area at 19 μm2 and a higher porosity of 46% compared to the PVDF NF membrane, which has a mean pore area of 2 μm2 and 34% porosity. This means that more MB molecules can penetrate and come in contact with the active sites of the nanofiber surface of the PAN NF membrane. Furthermore, the higher aspect ratio of the PVDF NF membrane, which resulted in more clumping, may have also contributed to its lower adsorption capacities when compared to PAN NF membranes. The largest difference in adsorption capacity (36.87%) occurred at the initial concentration of 7 mg/L when the maximum adsorption capacity is also achieved.

Table 2
Adsorption capacity of PAN and PVDF at equilibrium contact time.

Initial Concentration, mg/L	PAN Adsorption Capacity (qe), mg/g	PVDF Adsorption Capacity (qe), mg/g	Difference, %
3	17.34	14.41	18.46
5	34.98	30.48	13.75
7	50.78	34.97	36.87
10	12.81	9.98	24.84
15	13.88	11.00	23.15

3.5. Adsorption isotherm

In Table 3, three adsorption isotherms were used to determine which model best conforms to the data gathered during experimentation. Isotherm models help provide a comprehensive idea about the adsorbent characteristics. These isotherms help illustrate if the adsorbent surface is homogeneous or heterogeneous. It also gives an idea on the appropriate type of adsorption mechanism involved, whether it be chemisorption or physisorption, as well as on the determination of the maximum adsorption capacity of the MB molecules for a given NF membrane [43].

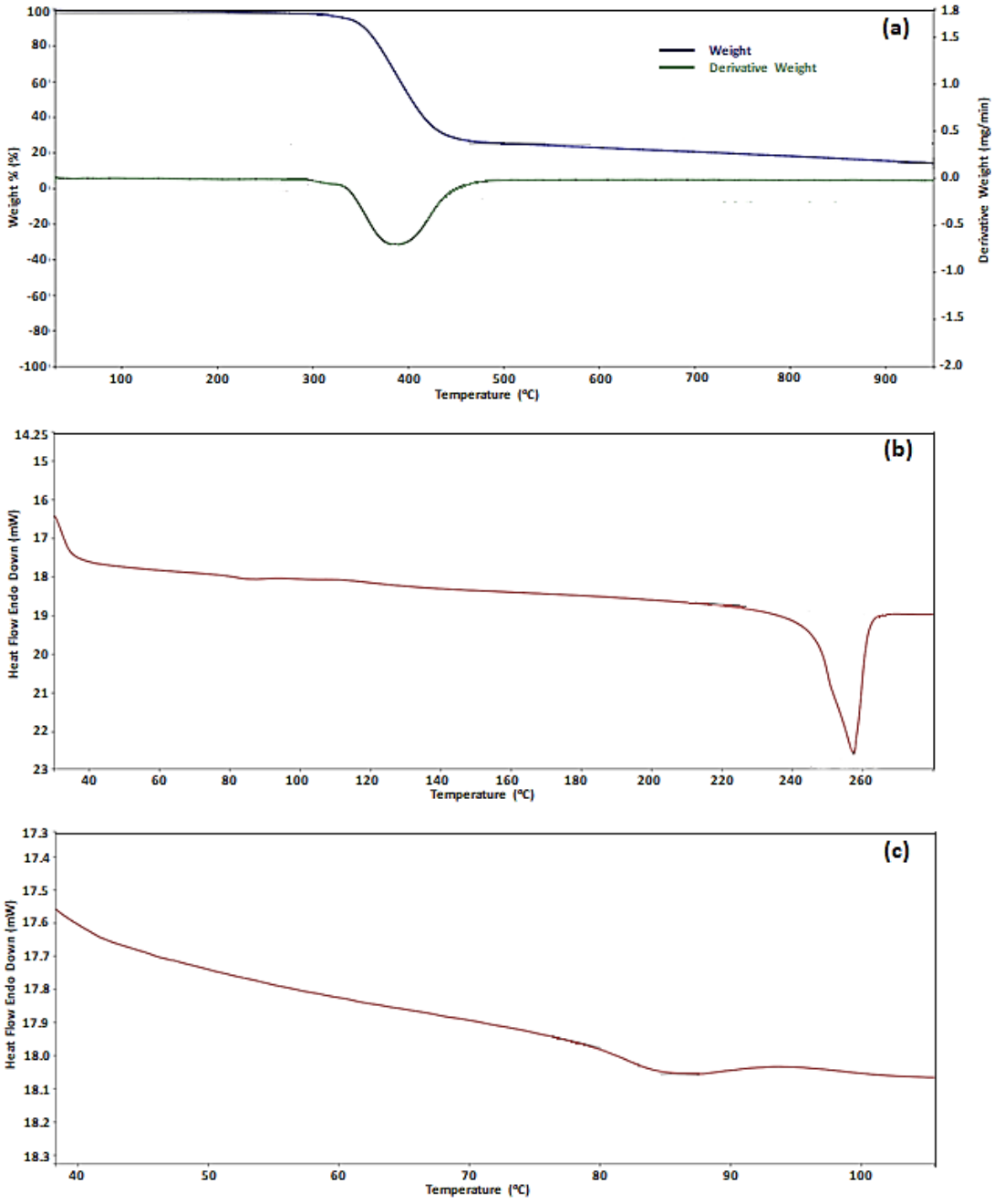

Fig. 7. (a) TG-DTG, (b) DSC, and (c) magnified glass transition curves of PAN nanofiber membrane.

Using Microsoft Excel 2016, an equation for each isotherm used were generated giving values for the slope (m), y-intercept (B) and the correlation value (R^2). The correlation value, R^2, was obtained for all isotherm models used in order to evaluate the appropriateness of the adsorbent used for MB dye adsorption [44]. Langmuir isotherm constants, q_m, and K_L were further calculated using equation 2, Freundlich isotherm constants n and K_F were obtained using equation 3 and Dubinin-Radushkevich isotherm constants, q_m, and E, were obtained using equations 5 and 7, respectively.

The Langmuir isotherm model (see Figure 9a) shows good fit of the adsorption data gathered for PAN NF membrane. This decision is based on the highest correlation coefficient, R^2 (see Table 3), compared to that of Freundlich isotherm and Dubinin-Radushkevich isotherm models. Such result implies that the adsorption mechanism involved is chemisorption [44] and a fixed number of active sites are present on NF surface membranes [6,45,46]. It also demonstrates that the MB molecules adsorbed forms a single layer [6,45,47]. However, the data yielded a negative value for the maximum adsorption capacity at -555.56 mg/g, which does not make physical sense.

The experimental data also highly correlates with the Freundlich isotherm model (see Figure 9b) but this model does not predict maximum adsorption capacity. However, it provides the value for n, which measures the intensity of the adsorption and K_F, which is an indicator of adsorption capacity [48]. The physisorption phenomenon is also more attributed to the Freundlich isotherm when correlation values are close to unity.

Although having the lowest correlation value compared to the two previously discussed, the batch adsorption data for PAN NF membrane also conforms well to the Dubinin-Radushkevich isotherm $R^2 = 0.917$ (see Figure 9c). Furthermore, this model gives a maximum adsorption capacity of 55.91 mg/g for the PAN NF membrane. Because of the negative adsorption obtained from the Langmuir isotherm, the adsorption capacity using Dubinin-Radushkevich isotherm was considered to be more realistic [49].

Table 3
Langmuir, Freundlich and Dubinin-Radushkevich adsorption isotherms parameters for MB adsorption of PAN and PVDF NF membrane.

PAN	R^2	m	B	q_m, (mg/g)	K_L	K_F	n	E (kJ/mol)
Langmuir isotherm	0.978	0.1131	-0.0018	-555.56	-0.01591	-	-	-
Freundlich isotherm	0.9486	1.086	2.1428	-	-	8.52	0.9208	-
Dubinin-Radushkevich isotherm	0.917	1.0x10-6	4.0238	55.91	-	-	-	0.707
PVDF	**R^2**	**m**	**B**	**q_m, (mg/g)**	**K**		**n**	**E (kJ/mol)**
Langmuir isotherm	0.9951	0.1529	-0.0027	-370.37	-0.01765	-	-	-
Freundlich isotherm	0.9905	0.9522	0.7779	-	-	0.4594	1.05	-
Dubinin-Radushkevich isotherm	0.9995	1.0x10-6	3.7856	44.06	-	-	-	0.707

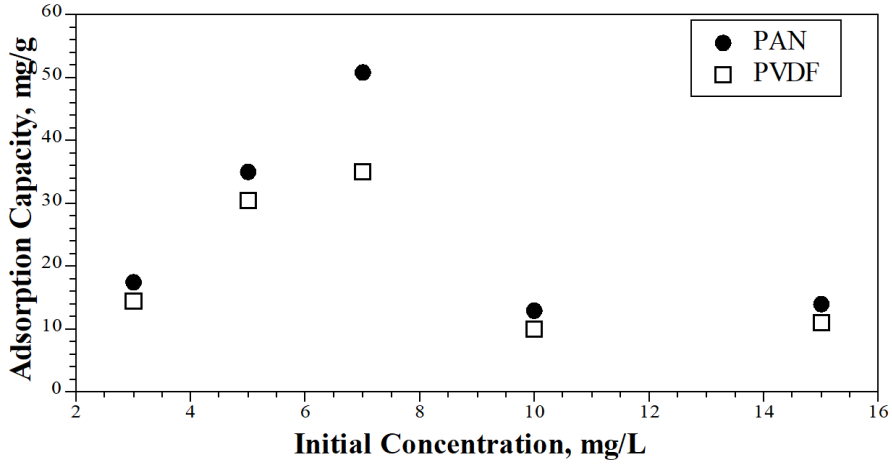

Fig. 8. Adsorption capacities of PAN and PVDF NF membranes at different initial concentrations of MB dye.

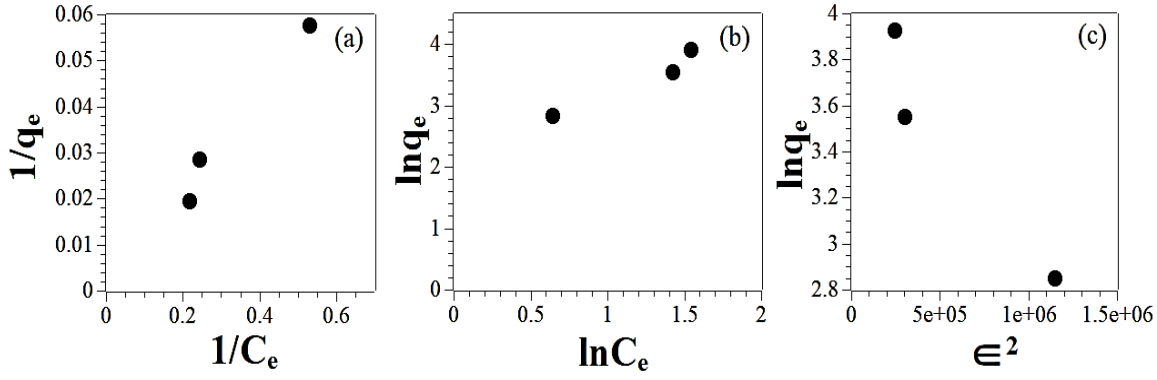

Fig. 9. Isotherm fitting using (a) Langmuir isotherm, (b) Freundlich isotherm and (c) Dubinin-Radushkevich using PAN membrane.

In PVDF NF membrane, the Dubinin-Radushkevich isotherm shows the best fit for its experimental data in Figure 10 with R^2 =0.9995. Such fit signifies that a pore-filling mechanism adsorption happens. And that a multilayer of adsorbate is also formed [24]. Furthermore, the mean free energy of adsorption (*E*) obtained is equal to 0.707 kJ/mol, which indicates a physisorption process. This free energy is the same type of force present is Van der Waals forces, which falls between 0.4 and 4 kJ/mol [50]. This isotherm model suggests that MB molecules form a multilayer on the PVDF nanofiber membrane's surface. The multilayer adsorption may possibly be formed as well. Such formation is caused by the agglomeration of MB molecules as face-to-face dimers of methylene blue can form in dilute concentrations. Subsequently, formation of higher aggregates occurs eventually when dye concentration increases [51]. The maximum adsorption capacity of the PVDF NF membrane obtained using the Dubinin-Radushkevich isotherm is 44.06 mg/g.

The obtained maximum adsorption capacities of the pristine PAN and PVDF NF membrane using the Dubinin-Radushkevich isotherm model are 55.91 mg/g and 44.06 mg/g, respectively. These values are comparable or even higher when compared to the adsorption capacities of some NF membranes from different studies. However, the acquired maximum adsorption capacity of the PAN and PVDF NF membranes used here are significantly lower compared to the crosslinked sodium alginate NF membrane [52], electrospun water-insoluble β-cyclodextrin-based fibers [46], and solution blow spun PMMA (Poly (methyl methacrylate)) nanofibers [10]. One reason for the low q_m obtained in this study is that the NF membranes used were not modified and functionalized, unlike those in the other MB

adsorption studies. Most, if not all, of the adsorbent membranes, used in Table 4, are amended by calcination or by other forms of heat treatment. The modification of the NF adsorbents and functionalization of groups present on its surface increases the active sites available for binding with the MB molecules, therefore, increasing the capability of the NF membranes for adsorption [53].

3.6. Recyclability test of nanofiber membranes

It is important to take into consideration the capacity of the PAN and PVDF nanofiber membranes for recyclability. After the batch adsorption, the nanofiber membranes used were kept and isolated until they were dried. The isolation was carried out by placing them in a container free from any contaminants and was partially closed to allow moisture to escape from the nanofiber membranes. The dried membranes were transferred to transparent plastic pouches and each pouch was labeled according to the type of nanofiber membrane and methylene blue solution concentration. The solution concentration at which the nanofiber membranes have the highest adsorption capacity for both PAN and PVDF nanofiber membranes was used for the recyclability test. Hydrochloric acid (0.01M HCl) was used to increase the acidity of the dye for the methylene blue removal. The nanofiber membranes were subjected in an Erlenmeyer flask with 30 mL Hydrochloric acid and were agitated for 30 minutes.

Results show that after the second cycle of adsorption as membranes were post-recycled, the adsorption capacities of both nanofiber membranes were reduced. PAN and PVDF NF membranes' adsorption capacity after the second cycle of adsorption was reduced to 18.34 mg/g and 16.22 mg/g, respectively. The calculated recyclability efficiency of the PAN and PVDF NF membranes are 79.04% and 80.47%, respectively.

3.7. Feasibility study for the scale-up plant design

A scale-up plant design plan was proposed for a manufacturing facility for the production of PVDF nanofiber membranes. The design aims to develop microfiltration membranes by means of solution blow spinning in comparison to the currently available and used microfiltration membranes in the world market. The potential markets include North America, Europe, Asia-Pacific, Latin America and the Middle East. These markets are the leading countries that uses microfiltration membrane owing to the strict regulation implemented for safe drinking water, rise in need of wastewater treatment in dye-contaminated waters for adsorption, filtration, and desalination to cope up with the water shortage. The PVDF nanofiber membrane microfilters produced from the design will be sold in rolls having an area of 1.8 m^2 of dimensions 300 mm x 6 m, and has a pore size of 1.59 microns. Other general requirements for microfiltration membranes are summarized on Table 5.

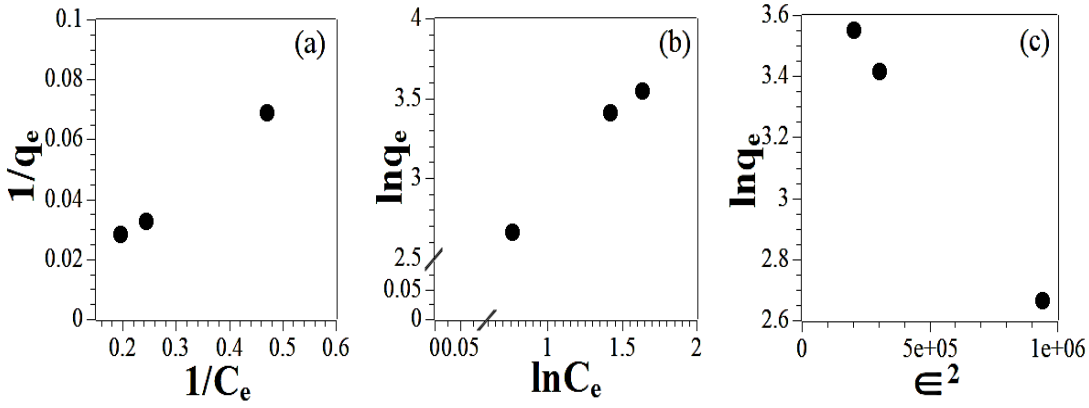

Fig. 10. Isotherm fitting using (a) Langmuir isotherm, (b) Freundlich isotherm and (c) Dubinin-Radushkevich models using PVDF membrane.

Table 4
Adsorption Capacities of Methylene blue dye used in different adsorbents with Langmuir Isotherm model.

Adsorbent	Amount (g)	q_m, (mg/g)	Reference
Electrospun p-cresol formaldehyde and polystyrene NF membrane	---	5.88 x 10^{-3}	[24]
Electrospun p-cresol formaldehyde and polystyrene NF membrane doped with zinc oxide nanoparticles	---	7.85 x 10^{-3}	[24]
Electrospun crosslinked gelatin/β- cyclodextrin NF membrane	0.01	47.4	[26]
Rice straws granular adsorbent	0.15	32.6	[43]
Electrospun Keratin Membrane	0.01	167	[54]
Crosslinked Sodium Alginate NF membrane	0.02	2357.87	[52]
Electrospun water-insoluble β-cyclodextrin-based fibers	0.014	826.45	[49]
Solution blow spun PMMA nanofibers	0.015	698.51	[10]
Electrospun PAN based activated carbon	0.007	72.46	[6]
Electrospun PAN with EDA grafting	---	94.07	[5]
Electrospun PAN NF membrane	---	42.662	[5]
Electrospun PVDF NF membrane with PDA	0.01	917.4	[55]
Modified PVDF NF membrane incorporated with HAPNP and PVP	0.12	10.83	[56]
Pristine PVDF NF membrane	0.12	2.89	[56]
Uncalcined solution blow spun PAN NF membrane	0.00703	55.91	This study
Uncalcined solution blow spun PVDF NF membrane	0.0082	44.06	This study

The manufacture of the PVDF membrane for microfiltration is separated into three steps: solution preparation, product processing and air treatment (Figure 11). For the solution preparation, raw materials are mixed together at a desirable state. This is followed by product processing wherein the prepared solution is introduced in the Solution blow spinning unit to undergo a process called solution blow spinning which uses compressed air at a pressure of 4 bars in blowing the polymer solution which causes the solvents to evaporate and therefore forming fibers which are collected using PET (Poly ethylene terephthalate) substrate. The air that exits the Solution blow spinning unit will no longer be treated as it falls below the limits set by the EPA (Environmental Protection Agency), hence it will be released to the atmosphere.

The proposed manufacturing facility will have two main structures allotted for the administration and for the production comprising of sixteen facilities with a total area of 225 square meters (15m by 15m). The total annual production of the plant is 8,106 rolls, which are sold for PhP 4,312.19 per roll, which is 6.05% cheaper compared to what is sold on the world market. The result of the economic analysis showed that the total capital investment is PhP 43,446,000.00. The total production cost is equal to Php 21,184,630.00, which is contributed by the fixed costs, variable costs, plant overhead costs, and general expenses. The annual average net revenue is Php 13,770,013.51. The payback period for the original investment is 4 years. Additionally, according to the Monte Carlo analysis, the plant has a 52% chance of being economically profitable. The project was designed to produce PVDF nanofiber membranes for water treatment in an environmentally sustainable, safe and cost effective process with an annual capacity of 14,590.8 m^2, which is 0.63% of the total world gap (2,313,300 m^2) posed by the limited supply of PVDF nanofiber membranes in the world market.

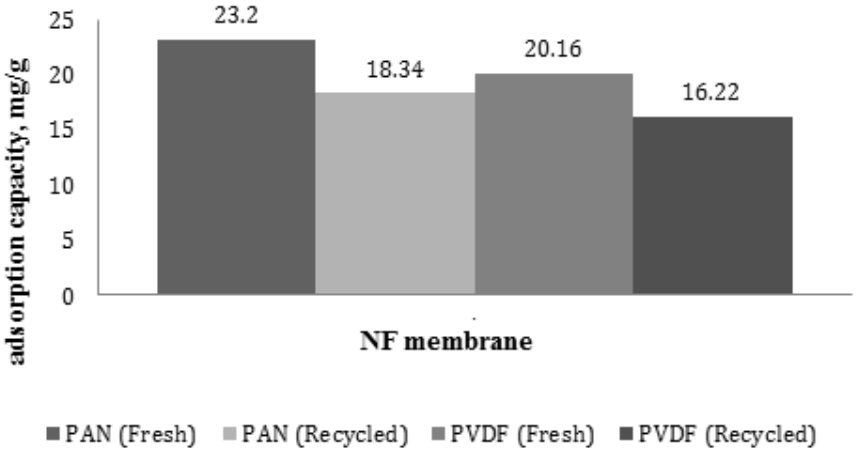

Fig. 10. Before and after recyclability test comparison of PAN and PVDF NF membranes at 5 mg/L and 2 minutes contact time.

Table 5
PVDF Microfiltration Membranes Specification.

Parameter	Standard Product-1 (Scienticfilters, 2020)	Standard Product-2 (Scienticfilters, 2020)	Product
Pore size, µm	1.00	3.00	1.59
Thickness, mm	0.085-0.12	0.085-0.12	0.09
Maximum temperature, (°C)	123	123	420
Width, mm	300	300	300
Length, m	6	6	6

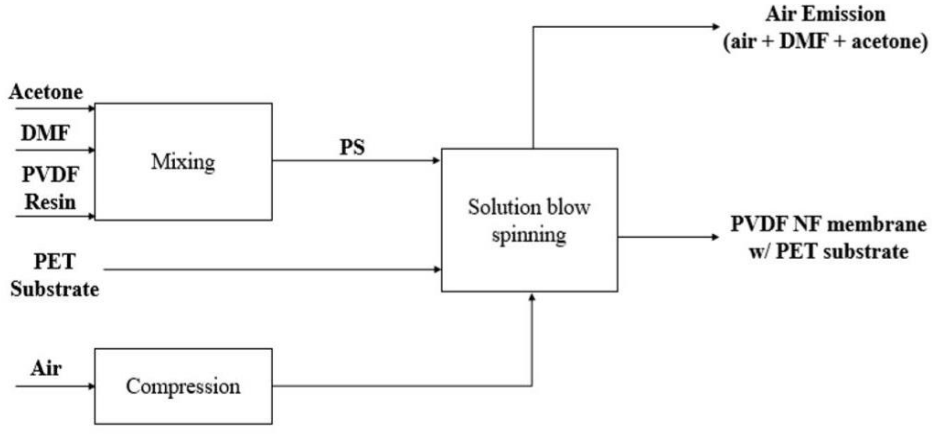

Fig. 11. Overall block flow diagram for PVDF nanofiber membrane production.

4. Conclusions

Varying the initial concentration has different effects on the behavior of the adsorption capacity of both PAN and PVDF nanofiber membranes. At low concentrations ranging from 3 to 7 mg/L, the adsorption capacity of both the nanofiber membranes increases until it reaches the highest adsorption capacity of 34.97 mg/g for the PVDF NF membrane and 50.78 mg/g for the PAN NF membrane. However, further increase of the initial concentration of the solution from 7 mg/L to 15 mg/L causes a decrease in the adsorption capacities of both NF membranes, which is attributed to the agglomeration of MB molecules in the solution as the initial concentration increases. Furthermore, rapid adsorption happens for the first minute of the adsorption process. However, after the initial minute, the adsorption continued to occur at a slower pace until it reached the state of equilibrium. The highest equilibrium adsorption capacity of the PAN NF membrane was obtained after 325.76 minutes, while it took 226.73 minutes for the PVDF NF membrane to accomplish the highest equilibrium adsorption capacity. PAN NF membranes also exhibited higher adsorption capacity than the PVDF nanofiber membrane for all levels of initial concentration of MB.

Both nanofiber membranes are proposed to conform to the Dubinin-Radushkevich adsorption isotherm models. Using this model, the predicted values for the maximum adsorption capacity of PAN and PVDF NF membranes are 55.91 mg/g and 44.06 mg/g, respectively. The model also implies that physisorption is the main adsorption mechanism for both type of nanofibers. Both pristine PAN and PVDF NF membranes produced by solution blow spinning therefore demonstrated satisfactory adsorption capacities. However, heat treatment and functionalization may still be employed in order to improve the adsorption performance of both nanofibers.

Acknowledgements

The researchers are grateful to the Balik Scientist Program of the Department of Science and Technology, Philippines (BSP-DOST) through the Philippine Council for Industry, Energy, and Emerging Technology Research and Development (PCIEERD) for the assistance and encouragement for research and development in the country, to the Chemical Engineering and Chemistry Departments of Xavier University- Ateneo de Cagayan laboratory personnel and its faculty, and to the Xavier University College of Engineering Parents and Faculty Association (XUCEPFA) for partially funding this project. Our gratitude is extended to Mr. Michael Dempsey for proofreading and English language editing this manuscript.

Conflict of interest

The authors declare that they have no known competing financial interests or personal relationships that could have appeared to influence the work reported in this paper.

Abbreviations

DMF	Dimethyl formamide
DSC	Differential scanning calorimetry
EDA	Ethylenediamine
EPA	Environmental Protection Agency
FTIR	Fourier transform infrared spectroscopy
HAPNP	Hydroxyapatite Nanoparticles
HCl	Hydrochloric acid
MB	Methylene blue
NaOH	Sodium Hydroxide
NF	Nanofiber
PAN	Poly (acrylonitrile)
PDA	Polydopamine
PET	Poly (ethylene terephthalate)
PMMA	Poly (methyl methacrylate)
PVDF	Poly (vinylidene fluoride)
PVP	Poly (vinylpyrrolidone)
SEM	Scanning electron microscopy
TGA	Thermogravimetric Analysis
TG-DTG	Thermogravimetric- derivative thermogravimetry

References

[1] F. M. D. Chequer, G. A. R. de Oliveira, E. R. A. Ferraz, J. C. Cardoso, M. V. B. Zanoni, D. P. de Oliveira, Textile Dyes: Dyeing Process and Environmental Impact, Eco-Friendly Textile Dyeing and Finishing. IntechOpen. 6 (2013) 151-176. DOI: 10.5772/53659.

[2] T. M. Albayati, A. A. Sabri, R. A. Alazawi, Separation of Methylene Blue as Pollutant of Water by SBS-15 in a Fixed-Bed Column, Arab J. Sci. Eng. 41 (2015) 2409-2415. DOI: 10.1007/s13369-015-1867-7.

[3] R. Karthik, R. Muthezhilan, A. J. Hussain, K. Ramalingam, V. Rekha, Effective Removal of methylene blue dye from water using three different low-cost adsorbents, J. Desalination and Water Treatment. 57 (2016) 10626-10631. DOI:10.1080/19443994.2015.1039598.

[4] G. Crini, E. Lichtfouse, Advantages and disadvantages of techniques use for wastewater treatment, Envi. Chem. Letters. 17 (2019) 145-155. DOI: 10.1007/s10311-018-0785-9.

[5] S. Haider, F. F. Binagag, A. Haider, A. Mahmood, N. Shah, W. A. Al-Masry, S. U. Khan, S. M. Ramay, Adsorption kinetic and isotherm of methylene blue, safranin T and rhodamine B onto electrospun ethylenediamine-grafted-polyacrylonitrile nanofibers membrane, J. Desalination and Water Treatment. 55 (2014) 1609-1619. DOI:10.1080/19443994.2014.926840.

[6] A. S. Ibupoto, U. A. Qureshi, F. Ahmed, Z. Khatri, M. Khatri, M. Maqsood, R. Z. Brohi, I. S. Kim, Reusable carbon nanofibers for efficient removal of methylene blue from aqueous solution, Chem. Eng. Res. Des. 136 (2018) 744-752. DOI:10.1016/j.cherd.2018.06.035.

[7] Z. Shen, G. P. Simon, Y. Cheng, Comparison of solution intercalation and melt intercalation of polymer-clay nanocomposites, Polym. 43 (2002) 4251-4260. DOI:10.1016/S0032-3861(02)00230-6.

[8] X. Zhang, Y. Lu, Centrifugal Spinning: An Alternative Approach to Fabricate Nanofibers at Hogh Speed and Low Cost, Polym. Rev. 54 (2014) 677-701. DOI: 10.1080/15583724.2014.935858

[9] D. D. S. Parize, M. M. Foschini, J. E. de Oliveira, A. P. Klamczynski, G. M. Glenn, J. M. Marconcini, L. H. C. Mattoso, Solution blow spinning: parameters optimization and effects on the properties of nanofibers from poly(lactic acid)/dimethyl carbonate solutions, J. Mater. Sci. 51 (2016) 4627-4638. DOI:10.1007/s10853-016-9778.

[10] L. A. Mercante, M. H. M. Facure, D. A. Locilento, R. C. Sanfelice, F. L. Migliorini, L. H. C. Mattoso, D. S. Correa, Solution Blow Spun PMMA Nanofibers Wrapped with Reduced Graphene Oxide as Efficient Dye Adsorbent, New J. Chem. 41 (2017) 9087-9094. DOI:10.1039/C7NJ01703K.

[11] J. E. Oliveira, L. H. C. Mattoso, W. J. Orts, E. S. Medeiros, Structural and Morphological Characterization of Micro and Nanofibers Produced by Electrospinning and Solution Blow Spinning: A Comparative Study, Adv. Mater. Sci. Eng. 1 (2013) 1-15, DOI:10.1155/2013/409572.

[12] M. Wojasinski, M. Pilarek, T. Ciach, Comparative studies of electrospinning and solution blow spinning processes for the production of nanofibrous poly(L-lactic acid) materials for biomedical engineering, Polish J. Chem. Tech. 16 (2014) 43-50. DOI: 10.2478/pjct-2014-0028.

[13] X. Zhuang, L. Shi, K. Jia, B. Cheng, W. Kang, Solution Blown Nanofibrous Membrane for Microfiltration, J. Membr. Sci. 429 (2013) 66-70. DOI:10.1016/j.memsci.2012.11.036.

[14] J. L. Daristotle, A. M. Behrens, A. D. Sandler, P. Kofinas, Review of the Principles and Applications of Solution Blow Spinning, ACS Appl. Mater. Interfaces. 8 (2016) 34951-34963. DOI:10.1021/acsami.6b12994. 34951-34963.

[15] A. M. C. Santos, M. F. Mota, R. S. Leite, G. A. Neves, E. S. Medeiros, R. R. Menezes, Solution bow spun titania nanofibers from solutions of high inorganic/organic precursor ratio, Ceram. Int. 44(2017) 1681-1689. DOI:10.1016/j.ceramint.2017.10.096.

[16] E. S. Medeiros, G. M. Glenn, A. P. Klamczynski,W. J. Orts, L. H. C. Mattoso, Solution Blow Spinning: A New Method to Produce Micro-and Nanofibers from Polymer Solutions, J. Appl. Polym. Sci. 113 (2009) 2322-2330. DOI:113:2322-2330.

[17] S. Subramanian, K. L. Tan, S. H. Lim, S. Ramakrishna, Electrospun Nanofibers for Air Filtration Applications, Procedia Eng. 75 (2014) 159-163. DOI:10.1016/j.proeng.2013.11034.

[18] J. Li, G. Song, J. Yu, Y. Wang, J. Zhu, Z. Hu, Preparation of Solution Blown Polyamic Acid Nanofibers and Their Imidization into Polyimide Nanofiber Mats, Nanomater. 7 (2017) 395-417. DOI:10.3390/nano7110395.

[19] G.C. Dadol, K.J.A. Lim, L.K. Cabatingan, N.P.B. Tan, Solution blow spinning–polyacrylonitrile–assisted cellulose acetate nanofiber membrane. Nanotechnol. 31 (2020) 345602. DOI: 10.1088/1361-6528/ab90b4.

[20] N.P.B. Tan, L.K. Cabatingan, K.J.A. Lim, Synthesis of TiO_2 nanofiber by solution blow spinning (SBS) method. Key Engineering Materials. DOI: 10.4028/www.scientific.net/kem.858.122

[21] N. P. B. Tan, S. S. Paclijan, H. N. M. Ali, C. M. J. Hallazgo, C. J.F Lopez, Y. C Ebora, Solution blow spinning (SBS) nanofibers for composite air filter masks. ACS Appl. Nano Mater. 2 (2019) 2475-2483. DOI: 10.1021/acsanm.9b00207.

[22] J. M. Salva, D. D. Gutierrez, L. A. Ching, P. M. Ucab, H. Cascon, N. P. B. Tan, Solution blow spinning (SBS) – assisted synthesis of well-defined carboxymethyl cellulose (CMC) nanowhiskers, Nanotechnol. 29 (2018) 50LT01, DOI: 10.1088/1361-6528/aae2fc.

[23] B. Ali Fil, C. Ozmetin, M. Korkmaz, Cationic Dye (Methylene Blue) Removal from Aqueous Solution by Montmorillonite, B. Korean Chem. Soc. 33 (2012) 3184-3190, DOI:10.5012/bkcs.2012.33.10.3184.

[24] W. J. Fendi, J. A. Naser, Adsorption Isotherms Study of Methylene Blue Dye on Membranes from Electrospun Nanofibers, Orient. J. Chem. 34 (2018) 2884-2894. DOI:10.13005/ojc/340628.

[25] N. Ayawei, A. N. Ebelegi, D. Wankasi, Modelling and Interpretation of Adsorption Isotherms, J. Chem. 2017 (2017) 1-11. DOI:10.1155/2017/3039817.

[26] Y. Chen, Y. Ma, W. Lu, Y. Guo, Y. Zhu, H. Lu, Y. Song, Environmentally Friendly Gelatin/β-Cyclodextrin Composite Fiber Adsorbents for the Efficient Removal of Dyes from Wastewater, Molecules. 23 (2018) 2473-2490. DOI:10.3390/molecules23102473.

[27] D. M. Ruthven, Principles of Adsorption and Adsorption Processes. Canada: John Wiley and Sons. 1984. DOI:10.1002/aic.690310335

[28] M. A. Al-Ghouti, D. A. Da'ana, Guidelines for the use and interpretation of adsorption isotherm models: A review, J. Hazard. Mater. 393 (2020) 122383-122482. DOI:10.1016/j.jhazmat.2020.122383

[29] C. J. Geankoplis, Transport Processes and Unit Operations, 3rd Edition, Boston, Allyn and Bacon, Prentice-Hall International, Inc. 1993. DOI: 10.1002/aic.690260236.

[30] A. O. Dada, A. P. Olalekan, A. Olatunya, Langmuir, Freundlich, Temkin and Dubinin–Radushkevich Isotherms Studies of Equilibrium Sorption of Zn^{2+} Unto Phosphoric Acid Modified Rice Husk, J. Appl. Chem. 3 (2012) 38-45. DOI: 10.9790/5736-0313845.

[31] M. T. Amin, A. A. Alazba, M. Shafiq, Adsorptive Removal of Reactive Black 5 from Wastewater Using Bentonite Clay: Isotherms, Kinetics and Thermodynamics, Sustainability. 7 (2015) 15302-15318. DOI:10.3390/su71115302.

[32] R. Vasireddi, J. Kruse, M. Vakili, S. Kulkarni, T. F. Keller, D. C. F. Monteiro, M. Trebbin, Solution blow spinning of polymer/nanocomposite micro-/nanofibers with tunable diameters and morphologies using a gas dynamic virtual nozzle, Sci. Rep. 9 (2019) 14297-14307. DOI:10.1038/s41598-019-50477-6.

[33] M. Zhou, K. Chen, X. Li, L. Liu, Q. Zeng, Y. Mo, L. Jin, L. Li, G. Su, J. Che, Y. Tian, Clumping Stability of Vertical Nanofibers on Surfaces, Langmuir. J. Am. Chem. Soc. 34 (2018) 11629-11636. DOI: 10.1021/acs.langmuir.8b02009.

[34] I. Karbownik, O. Rac-Rumijowska, M. Fiedot-Tobola, T. Rybicki, H. Teterycz, The Preparation and Characterization of Polyacrylonitrile-Polyaniline (PAN/PANI) Fibers, Mater. 12 (2019) 664-698. DOI:10.3390/ma12040664.

[35] D. R. Turner, A. J. Edwards, R. O. Piltz, Nitrile groups as hydrogen-bond acceptors in a donor-rich hydrogen-bonding network, CrystEngComm 14 (2012) 6447-6451. DOI:10.1039/C2CE26052B.

[36] B. Pant, G. P. Ojha, H. Y. Kim, M. Park, S. J. Park, Fly-ash-incorporated electrospun zinc oxide nanofibers: Potential material for environmental remediation, Environ. Pollut. 245 (2019) 163-172. DOI:10.1016/j.envpol.2018.10.122

[37] H. Bai, X. Wang, Y. Zhou, L. Zhang, Preparation and Characterization of Poly(vinylidene fluoride) Composite Membranes Blended With Nano-crystalline Cellulose, Prog. Nat. Sci: Mater. Int. 22 (2012) 250-257. DOI:10.1016/j.pnsc.2012.04.011.

[38] Z. Li, W. Kang, N. Wei, J. Qiu, C. Sun, B. Cheng, Preparation of a polyvinylidene fluoride tree-like nanofiber mat loaded with manganese dioxide for highly efficient lead adsorption, RSC Advances. 7 (2017) 8220-8229. DOI:10.1039/C6RA27865E

[39] I. Alarifi, A. Alharbi, W. Khan, A. Swindle, R. Asmatulu, Thermal, Electrical and Surface Hydrophobic Properties of Electrospun Polyacrylonitrile Nanofibers for Structural Health Monitoring. Materials, 8 (2015), 7017–7031. doi:10.3390/ma8105356

[40] A. Monahan, Thermal degradation of polyacrylonitrile in the temperature range 280–450°c. Journal of Polymer Science Part A-1: Polymer Chemistry, 4 (1966), 2391–2399. doi:10.1002/pol.1966.150041005

[41] A. Adnan, J. Shah, M. Jan, Effect of polyethylene terephthalate on the catalytic pyrolysis of polystyrene: Investigation of the liquid products. Journal of the Taiwan Institute of Chemical Engineers, 51 (2015), 96-102. 10.1016/j.jtice.2015.01.015.

[42] A. M. El-Wakil, W. M. Abou El-Maaty, O. Ahmed Abd Al-Ridha, Methylene Blue Dye Removal from Aqueous Solution Using Several Solid Stationary Phases Prepared from Papyrus Plant, J. Anal. Bioanal. Tech. 13 (2015) 1-7. DOI:10.4172/2155-9872.S13-003.

[43] N. Fathy, O. El-Shafey, L. Khalil, Effectiveness of Alkali-Acid Treatment in Enhancement the Adsorption Capacity for Rice Straw: The Removal of Methylene Blue Dye, J. Phys. Chem. 2013 (2013) 1-15. DOI:10.1155/2013/208087.

[44] H. Moussout, H. Ahlafi, M. Azza, H. Maghat, Critical of linear and non-linear equations of pseudo-first order and pseudo-second order kinetic model, Karbala International J. Mod. Sci. 4 (2018) 244-254. DOI:10.1016/J.KIJOMS.2018.04.001.

[45] J. Yongbin, H. Xiangyuan, Z. Yi, J. Hongbing, Chemisorption and Physical Adsorption Roles in Cadmium Biosorption by Chlamydomonas Reinhardtii, Chinese J. Population, Resour. Envi. 8 (2010) 54-58. DOI:10.1080/10042857.2010.10684991

[46] V. Meshko, L. Markovska, M. Mincheva, A. Rodrigues, Adsorption of Basic Dyes on Granular Activated Carbon and Natural Zeolite, Adsorption of Dyes, 35 (2001) 3357-3366. DOI: 10.1016/S0043-1354(01)00056-2.

[47] R. Zhao, Y. Wang, X. Li, B. Sun, C. Wang, Synthesis of β-Cyclodextrin-Based Electrospun Nanofiber Membranes for Highly Efficient Adsorption and Separation of Methylene Blue, Appl. Mater. Interfaces. 7 (2015) 26649-26657. DOI:10.1021/acsami.5b08403.

[48] Y. Zhang, J. Liu, X. Du, W. Shao, Preparation of reusable glass hollow fiber membranes and methylene blue adsorption. J. Eur. Ceram. Soc. 39 (2019) 4891-4900. DOI:10.1016/j.jeurceramsoc.2019.06.038.

[49] A. A. Inyinbor, F. A. Adekola, G. A. Olatunji, Kinetics, isotherms and thermodynamic modeling of liquid phase adsorption of Rhodamine B dye onto Raphia hookerie fruit epicarp. Water Resour. Ind. 15 (2016) 14-27. DOI:10.1016/j.wri.2016.06.001.

[50] L. Liu, X. Luo, L. Ding, S. Luo, Application of Nanotechnology in the Removal of Heavy Metal from Water, Nanomater. Rem. of Pollutants and Resour. Reutilization, 4 (2019) 83-147. DOI:10.1016/B978-0-12-814837-2.00004-4.

[51] S. L. Fornili, G. Sgroi, V. Izzo, Solvent isotope effect in the monomer-dimer equilibrium of methylene blue, J. Chem. Soc., Faraday Transactions. 1 (1981) 3049-3053. DOI:10.1039/F19817703049.

[52] Q. Wang, J. Ju, Y. Tan, L. Hao, Y. Ma, Y. Wu, H. Zhang, Y. Xia, K. Sui, Controlled Synthesis of Sodium Alginate Electrospun Nanofiber Membranes for Multi-occasion Adsorption and Separation of Methylene Blue, Carbohydr. Polym. 205 (2019) 125-134. DOI:10.1016/j.carbpol.2018.10.023.

[53] J. H. Kim, P. K. Park, C. H. Lee, H. H. Kwon, Surface modification of nanofiltration membranes to improve the removal of organic micro-pollutants (EDCs and PhACs) in drinking water treatment: Graft polymerization and cross-linking followed by functional group substitution, J. Membr. Sci. 321 (2008) 190-198. DOI:10.1016/j.memsci.2008.04.055.

[54] A. Aluigi, F. Rombaldoni, C. Tonetti, L. Jannoke, Study on Methylene Blue Adsorption on Keratin Nanofibrous Membrane, J. Hazard. Mater. 268 (2014) 156-165. DOI: 10.1016/j.jhazmat.2014.01.012.

[55] F. Ma, N. Zhang, X. Wei, J. Yang, Y. Wang, Z. Zhou, Blend-electrospun poly(vinylidene fluoride) polydopamine membranes Self-polymerization of dopamine and the excellent adsorption/separation abilities, J. Mater. Chem. 5 (2017) 14430-14443. DOI:10.1039/C7TA02845H

[56] J. Li, H. Zheng, H. Lin, B. Zhang, J. Wang, T. Li, Q. Zhang, Preparation of Three Dimensional Hydroxyapatite Nanoparticles Poly(vinylidene fluoride) Blend Membranes with Excellent Dye Removal Efficiency and Investigation of Adsorption Mechanism, Chinese J. Polym. Sci. 37 (2019) 1234-1247. DOI:10.1007/s10118-019-2271-7.